

Technical Advance

Mapping the Distribution of Neuroepithelial Bodies of the Rat Lung

A Whole-Mount Immunohistochemical Approach

Krishna P. Avadhanam, Charles G. Plopper,
and Kent E. Pinkerton

From the Department of Anatomy, Physiology, and Cell Biology, School of Veterinary Medicine, and the Institute of Toxicology and Environmental Health, University of California, Davis, Davis, California

We report an immunohistochemical method for mapping the distribution of neuroepithelial bodies (NEBs) in whole-mount preparations of the intrapulmonary airways. The lungs of 8- and 50-day-old male Sprague-Dawley rats were fixed with ethanol-acetic acid by intratracheal instillation. The major axial airway path of the infracardiac lobe was exposed and isolated by microdissection. NEBs were identified by calcitonin gene-related peptide immunoreactivity and their distribution mapped by generation and branch-point number. A distinct pattern was noted with greater prevalence of NEBs in proximal airway generations compared with more distal airways. No significant difference was noted in the distribution pattern or absolute number of NEBs between neonates and adults when compared by airway generation. NEBs were found more frequently on the ridges of the bifurcation than in other regions of the bifurcating airway wall. The ease of identification of total numbers of NEBs and their specific location by airway generation in whole-mount preparations of the bronchial tree completely removes the necessity of examining multiple sections and performing extensive morphometric procedures. Whole-mount airway preparations allow for the analysis and comparison of larger sample sizes per experimental

group without labor-intensive approaches. The application of this method should enhance our knowledge of the role of NEBs in lung development and in response to disease. (Am J Pathol 1997, 150:851–859)

Pulmonary neuroendocrine cells are specialized airway epithelial cells serving as intrapulmonary chemoreceptors^{1–3} and as a source of neuropeptides involved in regulation of lung growth and development.^{4,5} Neuroendocrine cells occur singly or in clusters (neuroepithelial bodies, NEBs). Due to their paucity within the airway tree, the identification, mapping, and systematic characterization of these cells have been difficult. They have been identified histologically by silver staining^{6,7} and periodic acid-Schiff-lead hematoxylin-positive staining^{8,9} as well as by formaldehyde-induced fluorescence.^{8,10} Immunohistochemical staining for general and specific neuropeptide markers is also a commonly used approach to identify neuroendocrine cells and NEBs.¹¹

Although immunohistochemical staining has been invaluable in defining the abundance and distribution of neuroendocrine cells in experimental and disease conditions, quantitative comparison among animals of various ages or experimental groups has been limited. In a previous study by Joad et al,¹²

Supported in part by the Center for Indoor Air Research, the University of California Tobacco-Related Disease Research Program, the NIEHS Center for Environmental Health Sciences (ES-05707), and a National Institutes of Health base grant to the California Regional Primate Research Center (RR00169).

Accepted for publication October 10, 1996.

Address reprint requests to Dr. Kent E. Pinkerton, ITEH, University of California, Davis, Davis, CA 95616-8615.

significant differences in neuroendocrine cell number per length of airway basal lamina were noted with long-term exposure to environmental tobacco smoke. However, localized changes in NEB frequency could not be determined. This was due to the inability to define airway branching history, airway position, or abundance of NEBs at airway branchpoints on random histological sections. NEBs have been demonstrated to be more frequent at airway branchpoints.^{8,13-15} However, the study by Joad et al¹² could not confirm whether NEBs had been increased specifically at bifurcations or simply at random sites along the intrapulmonary airways.

Serial section reconstruction of entire lung lobes in the past has been the only reliable approach to define the frequency and distribution of pulmonary neuroendocrine cells.¹⁶ Serial section analyses are highly laborious and time consuming. In addition, the effort required per sample makes this approach impractical for the large sample sizes associated with complex experimental studies. Reliable analysis of serial sections also requires sophisticated computer reconstruction strategies. Therefore, present histological techniques provide limited information on neuroendocrine cell distribution throughout the tracheobronchial tree and do not allow quantitative comparison among different generations, ages, species, and experimental groups.

A number of issues regarding neuroendocrine cells of intrapulmonary airways have not been completely addressed. How many NEBs are present per airway generation or on each airway bifurcation? Does every bifurcation have a NEB? Do neuroendocrine cell populations of the proximal and distal airways differ in abundance? Does the number and/or pattern of distribution of NEBs in neonates differ from that of adults?

The approach reported here was based on the rationale that to adequately address these questions requires a method that would 1) enhance the probability of identifying the precise distribution of NEBs in isolated airways, 2) increase the total numbers of NEBs evaluated per animal, and 3) facilitate experiments involving numerous animals without relying on the tedious and labor-intensive techniques of serial sectioning and computer-assisted reconstruction.

Materials and Methods

Animal Care and Tissue Preparation

Pregnant specific-pathogen-free Sprague-Dawley rats (Zivic-Miller Laboratories, Zelienople, PA) were housed and allowed food and water *ad libitum* ac-

cording to standard laboratory animal maintenance protocols. Dams were allowed to spontaneously give birth at 21 days gestational age. Only male rats were used in this study to minimize potential differences in NEB distribution based on gender. Pups were sacrificed at postnatal day (DPN) 8 with an overdose of sodium pentobarbital (intraperitoneally). After clearing the pulmonary circulation of blood with 0.01 mol/L phosphate-buffered saline (PBS), pH 7.4, ice-cold 95% ethanol/glacial acetic acid (99:1) was instilled intratracheally at 30 cm pressure for 1 hour. The lungs were removed from the thoracic cavity after 1 hour and transferred *en bloc* to ice-cold 70% ethanol. Lungs from five adult Sprague-Dawley males obtained separately from Zivic-Miller were also prepared as above and transferred to ice-cold 70% ethanol until microdissection.

Microdissection

The right infracardiac lobe was removed from the other lobes and the airway path was dissected out while being viewed under a dissecting microscope (Wild M8) as previously described.¹⁷ A single incision was made along the entire length of the axial pathway to the most distal airway generation. The entire circumference of the airway path was opened and spread flat. All blood vessels and parenchyma attached to the airway were carefully removed by blunt dissection while keeping the epithelium and submucosal connective tissue intact. All branches from the axial pathway were cut immediately distal to the branchpoint, so that the branching history remained obvious. Microdissected airways were placed in 70% ethanol until further use.

Reagents for Immunohistochemistry

Calcitonin gene-related peptide (CGRP) is a specific neuroendocrine marker that is highly expressed in rats and is ideal to identify and quantify NEBs.^{11,18} A polyclonal antibody against CGRP (Sigma Chemical Co., St. Louis, MO) produced in rabbit using synthetic rat CGRP conjugated to keyhole limpet hemocyanin was used.¹⁹ CGRP was obtained as delipidized whole antiserum and was 100% cross-reactive to rat CGRP. Biotinylated goat anti-rabbit IgG, goat serum, and ABC Vectastain Elite kits were obtained from Vector Laboratories (Burlingame, CA). Other reagents, solvents, buffers, and sera were obtained from Sigma or Fisher Scientific (Pittsburgh, PA).

Whole-Mount Immunohistochemistry

Airway segments were made permeable to antibodies by a series of dehydration/clearing/rehydration steps in increasing concentrations of ethanol (70, 95, and 100%), three changes of xylene, and decreasing concentrations of ethanol (100, 95, and 70%) for 15 minutes each. Permeabilization was accomplished by incubating the airway preparations in 0.3% Triton X-100 for 2 hours. Endogenous peroxidase activity was blocked by incubating the airways in 5 μ l/ml 30% H₂O₂ in methanol at room temperature for 1 hour. Washes between incubations were done for 15 minutes with several changes of 0.01 mol/L PBS, pH 7.4. Airways were drained and incubated in a blocking serum cocktail (5% goat serum, 5% rat serum, and bovine serum albumin in PBS) for 1 hour. Airways were incubated with anti-CGRP antiserum made in rabbit (1:500) for 40 hours followed by a 24-hour incubation with biotinylated goat anti-rabbit IgG (1:100). After overnight incubation with ABC peroxidase (Vectastain Elite Kit, Vector), CGRP-positive cells were labeled by diaminobenzidine reaction. Negative reagent control, with the primary antibody replaced by blocking serum, was run in parallel. The specificity of the antibody was determined on tissue sections before the whole-mount protocol, hence a CGRP antigen-absorbed negative control was not performed. Blocking serum without bovine serum albumin was used as primary and secondary antibody diluent. Antibody dilutions were made fresh for each immunostaining session. All washes less than 2 hours in length were carried out on an orbital shaker at room temperature in 12- or 24-well Falcon tissue culture plates (Fisher) based on the size of the airway preparation. Overnight incubations were done at 4°C under humidified conditions in tissue culture plates. The volume of the reagents used was dependent on the size of the airway isolation. Typically, 2 to 5 ml of reagents or antisera were used per well to completely immerse the airway preparation. Airways were not allowed to dry out at any stage of the immunohistochemical protocol. Immunostained airways were gently stretched on a slide with the epithelial side up and coverslipped, and NEBs were observed under bright-field illumination and imaged with an Olympus BH2 microscope equipped for differential interference contrast Nomarski.

Branching History

In the right infracardiac lobe of the rat lung, minor daughter airways branching from the main axial

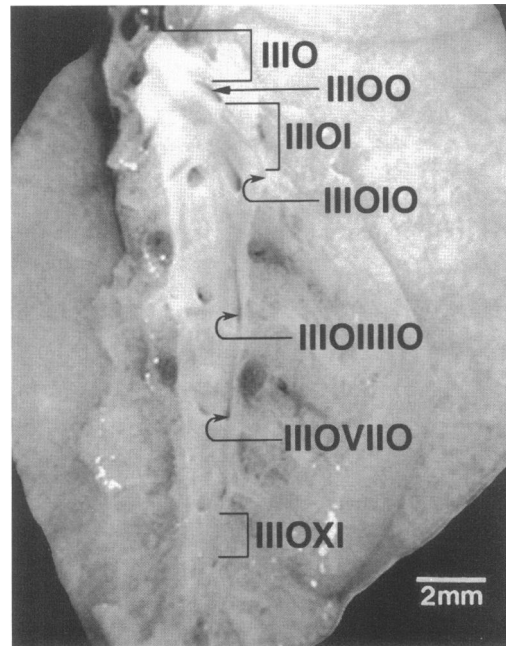


Figure 1. Microdissected axial pathway of the infracardiac lung lobe of a 50-day-old rat. The branching pattern of the axial pathway is designated by the binary classification system. Selected major daughter airway segments are indicated by brackets and minor daughter airway branches by arrows. Accordingly, the first major daughter airway segment of the right infracardiac lobe is designated as IIIIOI and the first minor daughter as IIIIOO. Scale bar, 2 mm.

pathway were typically found to occur in groups of three. Therefore, a numbering system for each branch arising from the axial pathway was designed. Beginning at the hilus, numbering proceeded distally along the axial pathway in a spiraling clockwise manner. In general, 20 to 22 generations of airways arising from the main axis were identified in each airway preparation of the right infracardiac lobe. In addition, each airway segment was designated using a binary classification system.¹⁷ Each minor daughter airway segment arising from the main axial pathway was designated by a 0, whereas the major daughter axial airway segment was designated by a 1. The binary classification system for a portion of the axial pathway of the right infracardiac lobe is illustrated in Figure 1.

Quantitation

Neuroendocrine cell distribution along the main axial airway path of three 8-day-old rats and five 50-day-old rats was analyzed in immunostained and slide-mounted airway preparations. Clusters of neuroendocrine cells (ie, NEBs) were noted and diagrammatically represented. Airways were divided into two regions: airway segments and bifurcation zones. The bifurcation zone was further divided into

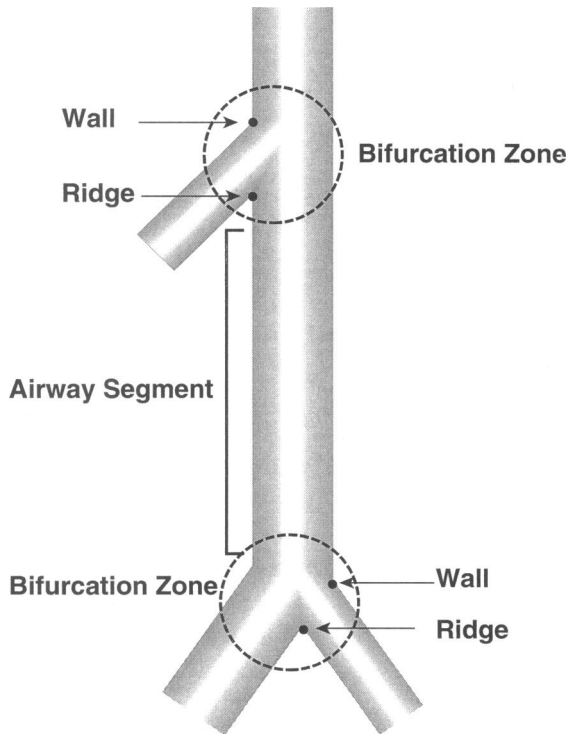


Figure 2. Identification of airway segments and bifurcation zones for whole-mount airway preparations. The airway between two branch-points is the airway segment. The region surrounding the branchpoint is designated as the bifurcation zone. Each bifurcation zone is subdivided into a ridge and wall based on the position within this zone.

1) the bifurcation ridge, or carinal point of the branching airway, and 2) the wall, or the remaining region of the bifurcation zone (Figure 2). Differences in the distribution of NEBs between corresponding intrapulmonary airway segments at the two ages were compared. NEBs present on the ridges and the walls of the bifurcation zone of the airway were also counted and their frequency compared. After counting, the airways were embedded in glycol methacrylate, cut into serial 2- μm -thick sections, lightly counterstained with methylene blue-basic fuchsin, and viewed under a light microscope (Olympus BH2) for confirmation of cells staining positively for CGRP.

Statistical Analysis

The average number of NEBs per airway segment and bifurcation zone was determined. Comparisons of NEB number per various airway segments, bifurcation zones, bifurcation ridges, and walls between and within the two age groups (8 and 50 DPN) were made using one-way analysis of variance followed by *post hoc* analyses using Scheffé's test or a Student's *t*-test as appropriate (Statview software ver-

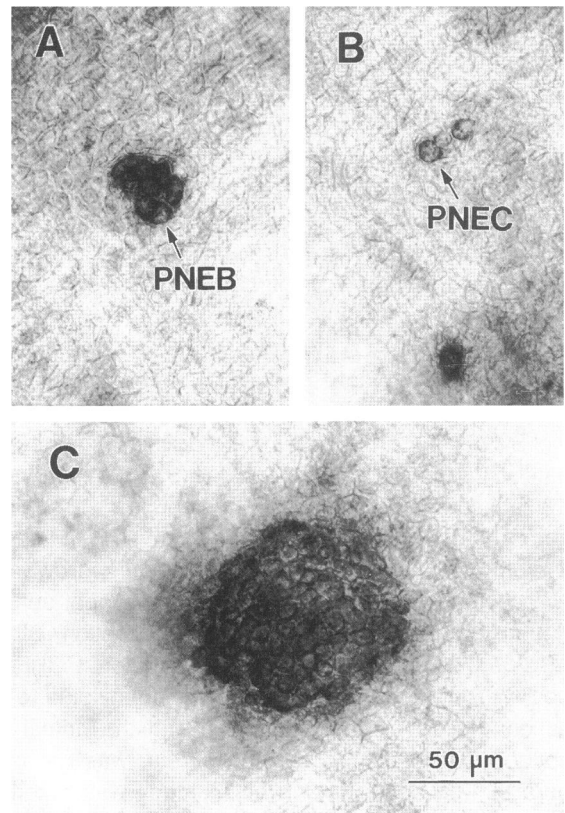


Figure 3. Differential interference contrast-Nomarski imaging of CGRP-positive airway epithelial cells in fixed and immunostained airway of 8-day-old neonatal rats. **A:** Cluster of pulmonary neuroendocrine epithelial cells (PNEB). **B:** Single CGRP-positive cells (PNEC) surrounded by unstained airway epithelial cells. **C:** Large NEBs, 10 to 12 cell diameters wide, were only occasionally found, compared with the more numerous NEBs of smaller cell number (A). Scale bar, 50 μm .

sion 4.5, Abacus Concepts, Berkeley, CA). Significance was considered at $P < 0.05$.²⁰

Results

Using avidin-biotin peroxidase immunohistochemistry on fixed and microdissected airways, cells that stained positive for CGRP were identified. Two types of CGRP-positive cells were noted in the epithelium: 1) clusters usually 3 to 4 cells in diameter (Figure 3A) and 2) single cells surrounded by unstained epithelial cells (Figure 3B). CGRP-positive cell clusters could be as few as 2 cells or as large as 10 to 12 cells in diameter (Figure 3C). Cell boundaries could be clearly identified using both transmitted light and differential interference contrast Nomarski optics by the appearance of a cobblestone arrangement due to the birefringence of the intervening plasma membranes of the adjacent cells. The epithelial layer was

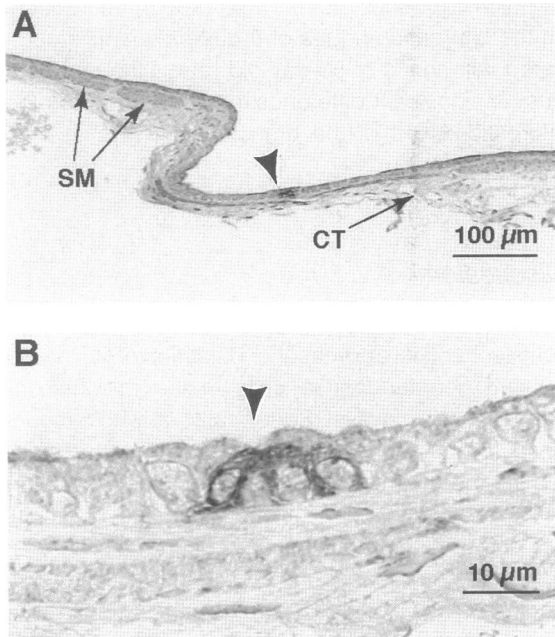


Figure 4. A: A whole-mount airway embedded in glycol methacrylate, sectioned, and counterstained with methylene blue-basic fuchsin. A continuous epithelial cell layer overlies smooth muscle bundles (SM) and connective tissue (CT). The location of a darkly stained NEB is indicated by an arrowhead. **B:** A serial section not counterstained shows this CGRP-positive NEB at higher magnification. Adjacent epithelial cells can be seen partially covering the stained neuroendocrine cells. Scale bars, 100 µm (A) and 10 µm (B).

intact as confirmed by the presence of a continuous sheet of translucent cells.

The positive staining of cells with CGRP antibody was confirmed in glycol methacrylate sections. Sections lightly counterstained with methylene blue-basic fuchsin demonstrated the presence of an intact epithelium along the entire length of the isolated airway. Within the lamina propria, smooth muscle bundles were observed along with connective tissue (Figure 4A). Parenchymal tissues were absent. At higher magnification, CGRP-positive cells were surrounded by unstained, nonciliated epithelial cells that partially covered the CGRP-positive cells. CGRP staining was confined to the cell cytoplasm, whereas the nuclei remained unstained (Figure 4B).

The distribution of NEBs in airway segments and along ridges and walls of the bifurcation zones was mapped for each airway isolation of each animal. A map for the entire airway isolation from a single 8-day-old animal laid flat and immunostained is shown diagrammatically in Figure 5. In this illustration, minor daughter airway branches arising from the axial pathway are indicated with numbered arcs from the proximal to distal portion of the bronchial tree. The designation according to binary classification of selected major daughter airway segments is

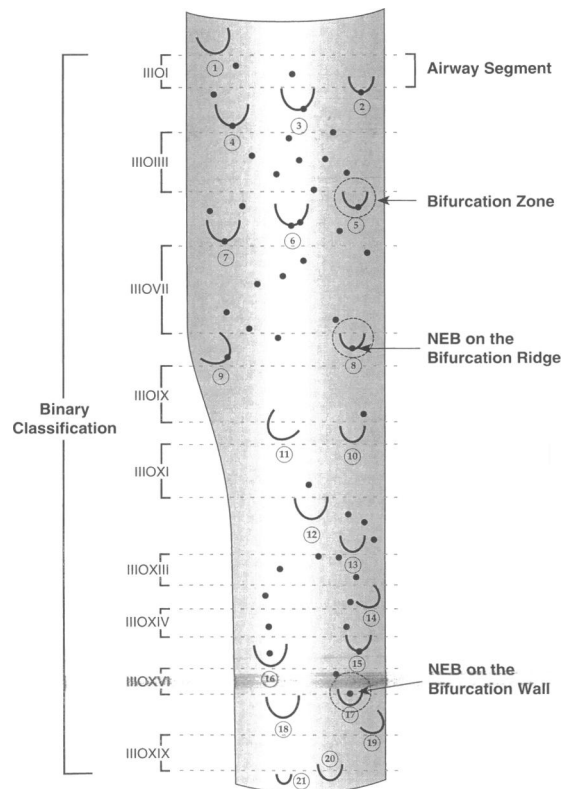


Figure 5. A map illustrating the distribution of NEBs of an immunostained whole mount of the entire circumference of the airway from a single 8-day-old rat lung. Numbered arcs indicate airway branches from the proximal to distal portion of the bronchial tree. Dotted lines demarcate airway segments labeled according to the binary classification system. The location of NEBs within this preparation is represented by the dots.

indicated. The dots represent the location of NEBs. The complete microdissected airway permitted mapping the precise distribution of NEBs throughout the airways. The whole-mount immunostained airways also allowed the absolute number of NEBs along the main axial pathway of the infracardiac lobe to be determined.

The distribution of NEBs in selected airway generations was compared at two ages (Figure 6). There was no significant difference in the number of NEBs per airway generation between both ages ($P = 0.78$, Scheffé's test). The pattern of NEB distribution was also found to be similar at both ages.

Differences were observed in the NEB distribution based on their location within the bifurcation zone, ie, the bifurcation ridge versus bifurcation wall. In the adult, there was on average at least one NEB on every bifurcation ridge (Figure 7B). The proportion of total NEBs at the bifurcation zones of the first 10 airway branches was 36% at 8 DPN and 35% at 50 DPN. More NEBs were found on bifurcation ridges than on bifurcation walls of the same bifurcation zone

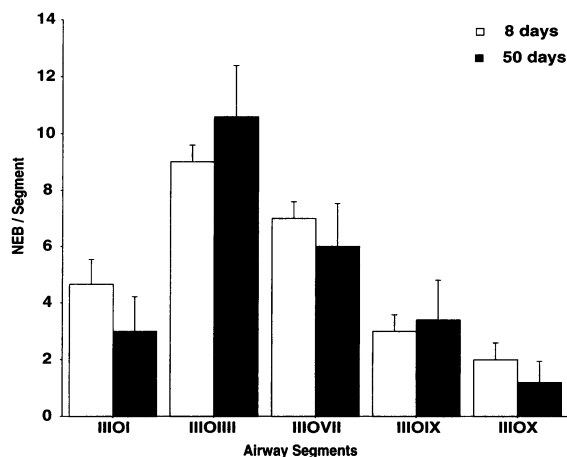


Figure 6. Bar graph comparing the average number of NEBs in specific airway segments of the bronchial tree at 8 and 50 DPN. Numbering of airway segments was according to the binary classification system. NEBs were identified by avidin-biotin peroxidase immunohistochemistry using an antibody against CGRP and viewed by light microscopy for quantitation. One-way analysis of variance confirmed that there was no significant difference between age groups in NEB frequency per segment ($P = 0.78$, Scheffé's test).

at both 8 (Figure 7A) and 50 days of age (Figure 7B);

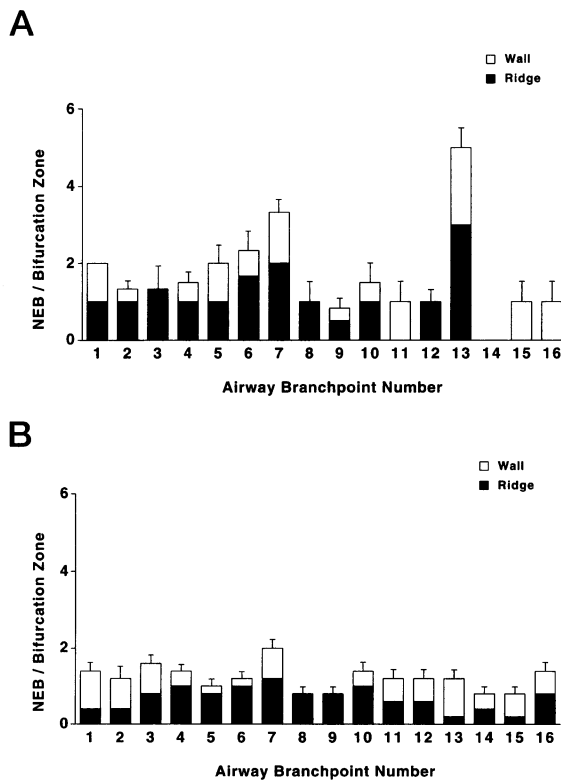


Figure 7. Bar graph comparing the average number of NEBs at each bifurcation zone subdivided into ridge and wall. Numbering of the branchpoints begins from the proximal to distal branches down the main axial airway path. NEBs were identified by avidin-biotin peroxidase immunohistochemistry using an antibody against CGRP and viewed by light microscopy for quantitation. NEBs were more frequent at the bifurcation ridges than on the bifurcation walls at both 8 DPN (A) and 50 DPN (B).

$P = 0.04$, Student's *t*-test). NEBs were more frequent on the bifurcation ridges of 8-day-old animals compared with those of 50-day-old rats, although there was no significant difference in NEB number on the bifurcation walls of the branching airways at both ages.

Discussion

The present communication reports a novel immunohistochemical approach for detection of NEBs and isolated neuroendocrine cells in the proximal intrapulmonary airways. Specifically, a whole-mount airway preparation method was developed to establish the three-dimensional topography and mapping of NEBs at different locations along the bronchial tree and within bifurcation zones (ie, ridge and wall). Pulmonary neuroendocrine cells consist of a specialized population of rare airway epithelial cells with neural and endocrine characteristics. Quantitative studies of pulmonary neuroendocrine cells in health and disease have been limited due to the need for large sample sizes and extensive analysis to obtain meaningful data. Studies by Gillan et al²¹ and Gosney et al²² show that neuroendocrine cells consist of less than 0.4% of the total airway epithelium in neonates and less than 0.02% in adults. The lungs of neonates have previously been reported to have a high abundance of neuroendocrine cells.^{23,24} In this study, 8- and 50-day-old rats were used to map and compare the distribution of NEBs. Neuroendocrine cells were not counted but were found to be numerous at both ages.

Whole-mount preparations have been used previously for immunohistochemical staining of nerves and specific cell types in the gastrointestinal tract,^{25,26} vasculature,²⁷ and retina²⁸ where spatial information about these structures in a complicated organ system is needed. The use of the entire specimen rather than histological sections for labeling antigenic markers of interest is the unique feature of whole-mount immunohistochemistry. Although immunostaining of whole-mount specimens is time consuming, it provides a quicker and more comprehensive analysis of the isolated and stained airway tree than can be done with immunohistochemistry on random paraffin sections. Attempts to apply this technique to the lung have been limited to the innervation of trachea, extrapulmonary bronchi, and intrapulmonary airways.^{29,30} In the past, a major problem of immunohistochemical analysis of whole-mount preparations of intact intrapulmonary airway epithelium has been nonspecific trapping of the la-

bel in the parenchyma surrounding the airway wall. Such interference is completely eliminated with this method of tissue preparation and staining. To the best of our knowledge, the present study is the first time that NEBs have been mapped in intact whole-mount preparations of the airways.

Using this method to map the distribution of NEBs, we found that almost all bifurcations have at least one NEB. It is also noteworthy that, within the bifurcation zone, more NEBs were observed on the ridge than on the wall. Based on our study, the proportion of total NEBs present at the bifurcations of the first 10 airway branches is 36% at 8 days and 35% at 50 days of age. Based on serial section analysis of a single hamster lung, Hoyt reported that 20% of the neuroendocrine cells were at the bifurcation.¹⁴ Based on airflow characteristics, the bifurcation ridge is likely to be a region of higher interception and deposition of inhaled particles and can be conjectured as an appropriate location for intrapulmonary chemoreceptors.³¹

Using the whole-mount airway approach, we found that the numbers of NEBs vary among various airway generations in the tracheobronchial tree. This observation is especially relevant based on the findings of Hoyt et al, using serial sections, that neuroendocrine cells differentiate centrifugally down the airway tree.^{14,32} In addition, we noted that NEBs were more numerous in the proximal airway segments compared with the more distal airways as was also found by Hoyt and colleagues in a single hamster lung reconstruction.^{14,32} Whole-mount immunohistochemistry also provides the advantage of mapping NEB distribution in major *versus* minor daughter airways. The abundance and pattern of distribution of NEBs in the same airway generation of both neonates and adults can also be compared with ease in whole-mount preparations. Several studies demonstrate that NEBs decrease in number with age.^{10,16,22,33-40} This reduction in NEBs with age may be an artifact due to a constant number of NEBs in rapidly expanding airways. This is especially plausible as extensive lung development occurs in humans⁴¹ and rats⁴² postnatally. Although the total number of NEBs is the same or slightly increased, in random lung sections there appears to be a decrease in the relative density of NEBs and isolated neuroendocrine cells in the epithelium due to expansion of the non-neuroendocrine epithelial cell compartment after birth.^{10,14,16,32} Our method substantiates observations of the latter studies and contradicts studies showing a reduction in neuroendocrine cell frequency with increasing age. A major advantage of this method is its applicability to stud-

ies involving large sample size without compromising the quality of analysis. As a large sample size is feasible using this method, it can be extended to studies with various test conditions using statistically valid numbers of animals. The method is highly reproducible, easy to perform, and can be rapidly done on numerous preparations.

Whole-mount immunohistochemistry clearly defines the branching history and allows counting of the absolute numbers of NEBs. This method facilitates a number of observations on the distribution pattern of neuroendocrine cells. Ease of identification, and quantitation of the number of NEBs per airway generation or bifurcation zone makes this method useful in identifying site-specific changes in the distribution of NEBs. Variability in the distribution of the NEBs of contiguous airway generations, in different airway segments, at different bifurcations, and within a single bifurcation zone can be clearly noted in airway isolations. This method confirms the variation in size of the NEBs (Figure 3) and also allows for determination of changes in NEB distribution with age (Figures 6 and 7). This study did not address the question of whether there is a trend toward larger NEBs either proximally or distally.

In conclusion, this approach should prove useful in evaluating the size, number, and distribution of pulmonary neuroendocrine cells throughout the airway tree for different airway generations, ages, mammalian species, and test conditions. Intrapulmonary airway epithelium can be surveyed for rare cell types that are difficult to study in randomly selected paraffin sections. This technique can be extended to monitor changes in NEB populations after exposure to hypoxia and air pollutants and in different airway disease models with a precise knowledge of the branching history of the airway in which they are found. This method may also prove useful in double-labeling techniques using cell cycle markers in conjunction with neuroendocrine markers to define the role of neuroendocrine cells in the proliferation of airway epithelium.⁴³ The technique can be modified to study alterations in other airway epithelial cell populations under experimental conditions and subsequent injury/repair processes using fixed and microdissected airway segments.

Acknowledgments

We thank Janice L. Peake and Adam A. Elliot for technical assistance.

References

1. Lauweryns JM, Peuskens JC: Neuro-epithelial bodies (neuroreceptor or secretory organs?) in human infant bronchial and bronchiolar epithelium. *Anat Rec* 1972, 172:471–481
2. Lauweryns JM, Cokelaere M: Intrapulmonary neuro-epithelial bodies: hypoxia-sensitive neuro(chemo)receptors. *Experientia* 1973, 29:1384–1386
3. Youngson C, Nurse C, Yeger H, Cutz E: Oxygen sensing in airway chemoreceptors. *Nature* 1993, 365:153–155
4. Sunday ME, Hua J, Reyes B, Masui H, Torday JS: Anti-bombesin monoclonal antibodies modulate fetal mouse lung growth and maturation *in utero* and in organ cultures. *Anat Rec* 1993, 236:25–34
5. King KA, Torday JS, Sunday ME: Bombesin and [Leu8]phyllolitorin promote fetal mouse lung branching morphogenesis *via* a receptor-mediated mechanism. *Proc Natl Acad Sci USA* 1995, 92:4357–4361
6. Tateishi R: Distribution of argyrophil cells in adult human lungs. *Arch Pathol* 1973, 96:198–202
7. Sonstegard K, Wong V, Cutz E: Neuro-epithelial bodies in organ cultures of fetal rabbit lungs: ultrastructural characteristics and effects of drugs. *Cell Tissue Res* 1979, 199:159–170
8. Sorokin SP, Hoyt RF Jr: Development of neuroepithelial bodies and solitary endocrine cells in fetal rabbit lungs. II. Nonspecific esterase as an indicator of early maturation. *Exp Lung Res* 1982, 3:261–272
9. Carabba VH, Sorokin SP, Hoyt RF Jr: Development of neuroepithelial bodies in intact and cultured lungs of fetal rats. *Am J Anat* 1985, 173:1–27
10. Redick ML, Hung KS: Quantitation of pulmonary neuroepithelial bodies in pre- and postnatal rabbits. *Cell Tissue Res* 1984, 238:583–587
11. Polak JM, Becker KL, Cutz E, Gail DB, Goniakowska-Witalinska L, Gosney JR, Lauweryns JM, Linnoila I, McDowell EM, Miller YE, Scheuermann DW, Springall DR, Sunday ME, Zaccane G: Lung endocrine cell markers, peptides, and amines. *Anat Rec* 1993, 236:169–171
12. Joad JP, Ji C, Kott KS, Bric JM, Pinkerton KE: *In utero* and postnatal effects of sidestream cigarette smoke exposure on lung function, hyperresponsiveness, and neuroendocrine cells in rats. *Toxicol Appl Pharmacol* 1995, 132:63–71
13. Cho T, Chan W, Cutz E: Distribution and frequency of neuro-epithelial bodies in post-natal rabbit lung: quantitative study with monoclonal antibody against serotonin. *Cell Tissue Res* 1989, 255:353–362
14. Hoyt RF Jr, Sorokin SP, Feldman H: Small-granule (neuro)endocrine cells in the infracardiac lobe of a hamster lung: number, subtypes, and distribution. *Exp Lung Res* 1982, 3:273–298
15. Cutz E, Chan W, Sonstegard KS: Identification of neuro-epithelial bodies in rabbit fetal lungs by scanning electron microscopy: a correlative light, transmission and scanning electron microscopic study. *Anat Rec* 1978, 192:459–466
16. Sarikas SN, Hoyt RF Jr, Sorokin SP: Small-granule APUD cells in relation to airway branching and growth: a quantitative, cartographic study in Syrian golden hamsters. *Anat Rec* 1985, 213:410–420
17. Plopper CG: Structural methods for studying bronchiolar epithelial cells. *Models of Lung Disease: Microscopy and Structural Methods*. Edited by J Gil. New York, Marcel Dekker, 1990, pp 537–559
18. Cadieux A, Springall DR, Mulderry PK, Rodrigo J, Ghatei MA, Terenghi G, Bloom SR, Polak JM: Occurrence, distribution, and ontogeny of CGRP immunoreactivity in the rat lower respiratory tract: effect of capsaicin treatment and surgical denervations. *Neuroscience* 1986, 19:605–627
19. Skofitsch G, Jacobowitz DM: Calcitonin gene-related peptide: detailed immunohistochemical distribution in the central nervous system. *Peptides* 1985, 6:721–745
20. Fisher L, van Belle G: *Biostatistics: A methodology for the health sciences*. Series title: Wiley series in probability and mathematical statistics. Applied Probability and Statistics. Edited by L Fisher. New York, J Wiley, 1993, pp 145–146, 418–431
21. Gillan JE, Pape KE, Cutz E: Association of changes in bombesin immunoreactive neuroendocrine cells in lungs of newborn infants with persistent fetal circulation and brainstem damage due to birth asphyxia. *Pediatr Res* 1986, 20:828–833
22. Gosney JR, Sissons MC, Allibone RO: Neuroendocrine cell populations in normal human lungs: a quantitative study. *Thorax* 1988, 43:878–882
23. Hoyt RF Jr, McNelly NA, Sorokin SP: Dynamics of neuroepithelial body (NEB) formation in developing hamster lung: light microscopic autoradiography after ^3H -thymidine labeling *in vivo*. *Anat Rec* 1990, 227:340–350
24. Nakatani Y: Pulmonary endocrine cells in infancy and childhood. *Pediatr Pathol* 1991, 11:31–48
25. Pearson GT: Structural organization and neuropeptide distributions in the equine enteric nervous system: an immunohistochemical study using whole-mount preparations from the small intestine. *Cell Tissue Res* 1994, 276:523–534
26. Wells DG, Talmage EK, Mawe GM: Immunohistochemical identification of neurons in ganglia of the guinea pig sphincter of Oddi. *J Comp Neurol* 1995, 352:106–116
27. Maynard KI, Ogilvy CS: Patterns of peptide-containing perivascular nerves in the circle of Willis: their absence in intracranial arteriovenous malformations. *J Neurosurg* 1995, 82:829–833
28. Lammerding-Koppel M, Thier P, Koehler W: Morphology and mosaics of VIP-like immunoreactive neurons in the retina of the rhesus monkey. *J Comp Neurol* 1991, 312:251–263
29. Baluk P, Nadel JA, McDonald DM: Substance P-immunoreactive sensory axons in the rat respiratory tract: a quantitative study of their distribution and role in neu-

- rogenic inflammation. *J Comp Neurol* 1992, 319:586–598
30. Sparrow MP, Warwick SP, Everett AW: Innervation and function of the distal airways in the developing bronchial tree of fetal pig lung. *Am J Respir Cell Mol Biol* 1995, 13:518–525
 31. Lippmann M, Schlesinger RB: Interspecies comparison of particle deposition and mucociliary clearance in the tracheobronchial airways. *J Toxicol Environ Health* 1984, 13:441–469
 32. Hoyt RF Jr, Feldman H, Sorokin SP: Neuroepithelial bodies (NEB) and solitary endocrine cells in the hamster lung. *Exp Lung Res* 1982, 3:299–311
 33. Hage E, Hage J, Juel G: Endocrine-like cells of the pulmonary epithelium of the human adult lung. *Cell Tissue Res* 1977, 178:39–48
 34. Hage E: Morphology and histochemistry of the normal and abnormal pulmonary endocrine cell. *The Endocrine lung in Health and Disease*. Edited by KL Becker, AF Gazdar. Philadelphia, Saunders, 1984, pp 193–209
 35. Johnson DE, Lock JE, Elde RP, Thompson TR: Pulmonary neuroendocrine cells in hyaline membrane disease and bronchopulmonary dysplasia. *Pediatr Res* 1982, 16:446–454
 36. Johnson DE, Kulik TJ, Lock JE, Elde RP, Thompson TR: Bombesin-, calcitonin-, and serotonin-immunoreactive pulmonary neuroendocrine cells in acute and chronic neonatal lung disease. *Pediatr Pulmonol*, 1985, 1:S13–S20
 37. Tsutsumi Y, Osamura RY, Watanabe K, Yanaihara N: Immunohistochemical studies on gastrin-releasing peptide- and adrenocorticotrophic hormone-containing cells in the human lung. *Lab Invest* 1983, 48:623–632
 38. Tsutsumi Y, Osamura RY, Watanabe K, Yanaihara N: Simultaneous immunohistochemical localization of gastrin releasing peptide (GRP) and calcitonin (CT) in human bronchial endocrine-type cells. *Virchows Arch A Pathol Anat Histopathol* 1983, 400:163–171
 39. DiAugustine RP, Sonstegard KS: Neuroendocrine like (small granule) epithelial cells of the lung. *Environ Health Perspect* 1984, 55:271–295
 40. Sunday ME, Kaplan LM, Motoyama E, Chin WW, Spindel ER: Gastrin-releasing peptide (mammalian bombesin) gene expression in health and disease. *Lab Invest* 1988, 59:5–24
 41. Burri PH: The postnatal development and growth of the human lung. II. Morphology. *Respir Physiol* 1987, 67: 247–267
 42. Burri PH: The postnatal growth of the rat lung. III. Morphology. *Anat Rec* 1974, 180:77–98
 43. Hoyt RF Jr, McNelly NA, McDowell EM, Sorokin SP: Neuroepithelial bodies stimulate proliferation of airway epithelium in fetal hamster lung. *Am J Physiol* 1991, 260:L234–L240